ATMOSPHERIC SCIENCE

New generation of U.S. satellite microwave sounder achieves high radiometric stability performance for reliable climate change detection

Cheng-Zhi Zou[1]*, Mitchell D. Goldberg[2], Xianjun Hao[3]

Observations from the satellite microwave sounders play a vital role in measuring the long-term temperature trends for climate change monitoring. Changes in diurnal sampling over time and calibration drift have been the main sources of uncertainties in the satellite-measured temperature trends. We examine observations from the first of a series of U.S. new generation of microwave sounder, the Advanced Technology Microwave Sounder (ATMS), which has been flying onboard the National Oceanic and Atmospheric Administration (NOAA)/NASA Suomi National Polar-orbiting Partnership (SNPP) environmental satellite since late 2011. The SNPP satellite has a stable afternoon orbit that has close to the same local observation time as NASA's Aqua satellite that has been carrying the heritage microwave sounder, the Advanced Microwave Sounding Unit-A (AMSU-A), from 2002 until the present. The similar overpass timing naturally removes most of their diurnal differences. In addition, direct comparison of temperature anomalies between the two instruments shows little or no relative calibration drift for most channels. Our results suggest that both SNPP/ATMS and Aqua/AMSU-A instruments have achieved absolute stability in the measured atmospheric temperatures within 0.04 K per decade. This uncertainty is small enough to allow reliable detection of the temperature climate trends and help to resolve debate on relevant issues. We also analyze AMSU-A observations onboard the European MetOp-A satellite that has a stable morning orbit 8 hours apart from the SNPP overpass time. Their comparison reveals large asymmetric trends between day and night in the lower- and mid-tropospheric temperatures over land. This information could help to improve climate data records for temperature trend detection with improved accuracy. The SNPP satellite will be followed by four NOAA operational Joint Polar Satellite System (JPSS) satellites, providing accurate and stable measurement for decades to come. The primary mission of JPSS is for weather forecasting. Now, with the added feature of stable orbits, JPSS observations can also be used to monitor changes in climate with much lower uncertainty than the previous generation of NOAA operational satellites.

INTRODUCTION

Accurate determination of long-term global temperature trends is critically important for the climate science community as well as the public to understand how anthropogenic greenhouse gas emissions have influenced global climate change. It also provides an observational record for validating climate model simulations of climate changes in the past, building confidence for the climate models to predict climate changes in the future. Such a capability will ultimately help society to develop informed policies on climate change mitigation and adaptation.

Although the primary mission of sun-synchronous, polar-orbiting environmental satellites is weather forecasting, providing most observations used in global forecasting models (*1*), polar-orbiting satellites have been playing a vital role in measuring temperature trends during the past few decades (*2*–*18*) owing to their global coverage and long-term continuity. However, satellite-derived temperature trends have been a subject of debate for nearly three decades. The first attempt to derive satellite-based atmospheric temperature trends was made in the early 1990s using observations from the Microwave Sounding Unit (MSU) onboard the National Oceanic and Atmospheric Administration (NOAA) Polar-orbiting Operational Environmental Satellite series (*2*). The MSU and its follow-on microwave sounders passively measure the upwelling radiances from the 50- to 60-GHz absorption band of the atmospheric oxygen in discrete frequency channels. The radiance measured by each frequency channel comes from a different layer of the atmosphere, depending on the strength of the absorption at that frequency. The relative contribution of temperatures at individual levels to the measured layer temperature is represented by a vertical weighting function, which is typically a bell-shaped curve peaking at certain level in the height coordinate (Fig. 1). The initial study (*2*) used MSU channel 2 with a frequency band catered at 53.74 GHz for temperature trend detection in the mid-troposphere. The same group also created a lower-tropospheric temperature time series from differences between the near-nadir and near-limb observations of MSU channel 2 (*3*). This study found near-zero trends during 1979–1990 in the lower- and mid-tropospheric temperatures, in contradiction to both the ground-based observational evidence that the surface temperature had been increasing during the same period (*4*) and the theoretical prediction that the global temperature near the Earth's surface shall be increasing due to increasing greenhouse gases such as the carbon dioxide in the atmosphere (*19*).

One explanation for this inconsistency was that the MSU channel 2 weighting function extended from the surface to the lower stratosphere (Fig. 1); hence, temperature trends derived from this channel contained contribution from the lower stratosphere that had been cooling during the same period of time. Removing this lower-stratospheric cooling effect resulted in warming trends in the satellite-derived mid-tropospheric temperature (*5*).

Lower-stratospheric contamination was not the only factor that caused the inconsistencies between the warming surface and the near-zero temperature trends in the lower and middle troposphere in the initial study. With more investigation, researchers found that residual biases remained after satellite data processing and these biases influence MSU-derived long-term trends. It is now well understood that four

[1]Center for Satellite Applications and Research, NOAA/NESDIS, College Park, MD 20740, USA. [2]Joint Polar Satellite System, NOAA/NESDIS, Lanham, MD 20706, USA. [3]Global Environment and Natural Resources Institute/Environmental Science and Technology Center, George Mason University, Fairfax, VA 22030, USA.
*Corresponding author. Email: cheng-zhi.zou@noaa.gov

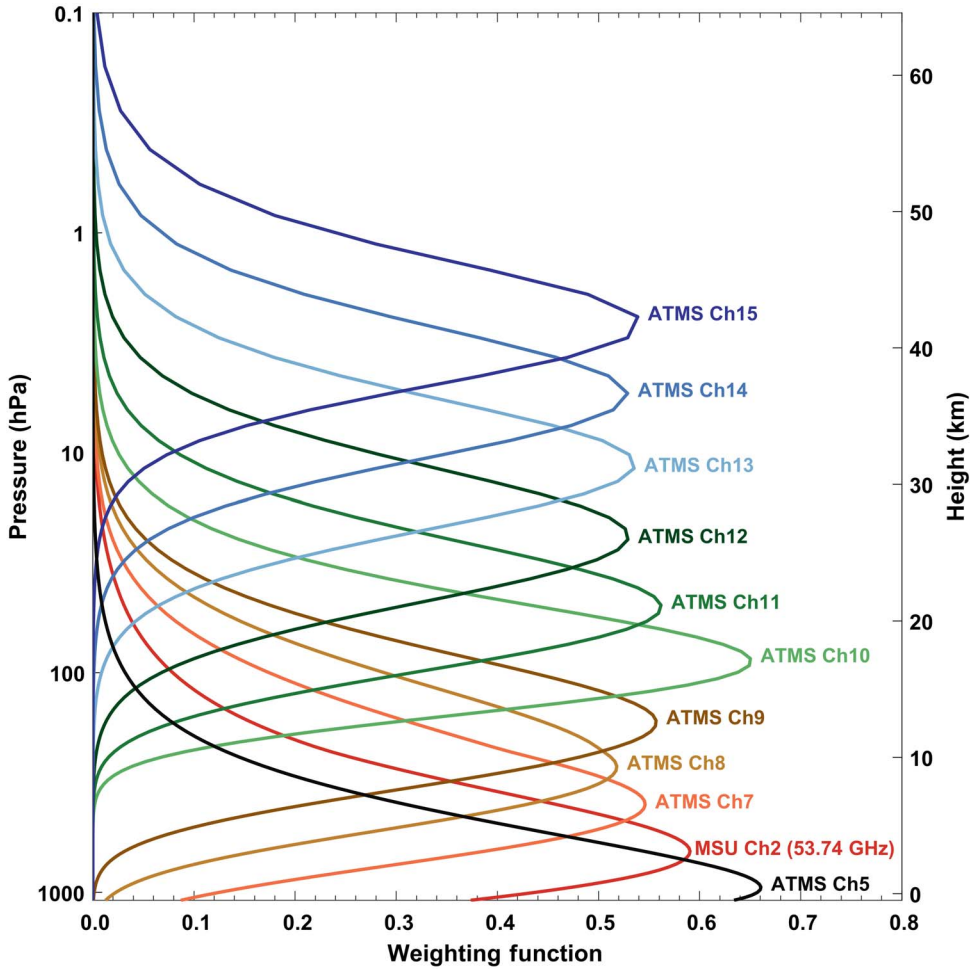

Fig. 1. Weighting functions of satellite microwave sounders. Weighting functions for MSU channel 2 and ATMS channels 5 to 15. The AMSU-A weighting functions are the same as those of the ATMS counterpart channels.

types of errors could result in spurious temperature trends from satellite observations. The first is the sampling error that occurs when different satellites sample Earth at different local times due to their deployment in different sun-synchronous orbits. This problem also afflicts individual satellites as their orbits drift with satellite aging (Fig. 2) caused by constant gravitational attraction from Earth. The magnitudes of temperature diurnal cycles in the lower and middle troposphere are large over the land area. If not or wrongly corrected, the temperature diurnal differences due to different observation time can become aliased with the long-term satellite time series, causing spurious trends in the satellite observations (*6*).

The second error source is the decrease in satellite orbital altitudes, which originates from drags on the spacecraft from the solar ultraviolet radiative heating (*7*). The orbital decay causes brightness temperatures from the satellite near-limb views to warm faster relative to those from the near-nadir views (*7*). For temperature of the lower troposphere, the different warming rates between the near-nadir and near-limb observations introduce a spurious cooling trend to the final time series. This effect is negligible for temperature of the mid-troposphere, which is derived from averages of the near-nadir views.

The third error source is from the satellite calibration, a process that converts the signals received by a satellite antenna in the form of electric voltage counts to radiances emitted by Earth that are used for geophysical applications. The designed calibration uncertainty estimate for satellite microwave sounders is 0.5 to 1 K. Constant calibration errors do not affect trend estimates because they are cancelled out by time derivative. However, calibration errors may drift over time due to changes in calibration nonlinearity (*8*–*10*). The calibration-drifting errors can be larger than the climate trend signals, which are on the order of 0.1 to 0.2 K per decade in the lower and middle troposphere (*9*–*14*). Calibration-drifting errors can cause two satellite records to drift away from each other with time, which inevitably leads to differences in their trend estimates. Recalibration aiming to remove these errors must be conducted in order for observations from different satellites to be able to reliably detect temperature trends (*8*–*14*).

The fourth error source is from changes in channel frequencies in different generations of the microwave sounders. The MSU was followed by the second generation of the microwave sounder, the Advanced Microwave Sounding Unit-A (AMSU-A), starting from 1998 until the present. The AMSU-A contains more channels, with their measurement extended from the surface to the upper stratosphere with higher spatial resolutions both horizontally and vertically than its predecessor, the MSU. However, channel frequencies in their counterpart channels are slightly different (Table 1), resulting in differences in samplings of the atmospheric layers. Researchers found drift over time in the biases between the last MSU satellite, the NOAA-14, and the first AMSU-A

satellite, the NOAA-15 (*13*), possibly due to a combination of calibration-drifting errors and channel frequency differences between them. In addition, channel frequencies may shift from their prelaunch specifications after satellite launch for the same MSU or AMSU-A instruments (*10*, *20*), causing sampling biases relative to other instruments of the same type. Bias removal algorithms must be developed to account for this type of error (*8*–*16*).

With efforts over more than two decades, researchers developed various algorithms for removing errors, as described above (*7*–*16*). With improved algorithms, satellite-derived tropospheric temperature trends show better agreement in the latest versions developed by different research groups compared to their earlier versions. Specifically, the mid-tropospheric temperature trends from two of three research groups agree with each other quite well (*17*, *18*). However, trend differences still exist due to differences in algorithms selected in developing temperature time series by different research groups.

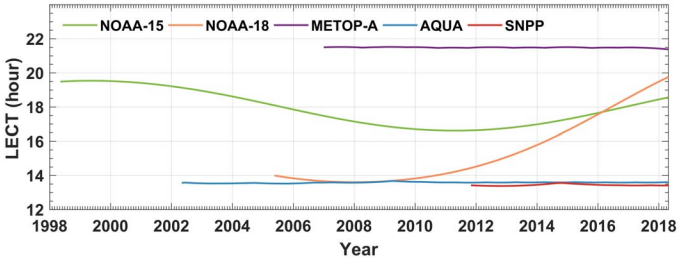

Fig. 2. Satellite local equator crossing time. Local equator crossing time (LECT) of the ascending orbits for Aqua, MetOp-A, and SNPP, in comparison with NOAA-15 and NOAA-18 satellites with an orbital drift. The descending and ascending orbits are 12 hours apart.

The situation has changed completely with the next-generation U.S. microwave sounder, the Advanced Technology Microwave Sounder (ATMS). The ATMS is currently being flown on the NOAA/NASA Suomi National Polar-orbiting Partnership (SNPP) satellite and the NOAA-20 [Joint Polar Satellite System-1 (JPSS-1) before launch] and to be flown on future JPSS platforms. The ATMS is a total power cross-track radiometer with 22 channels, combining all the channels of the heritage sensors into a single sensor that spans from 23 to 183 GHz for atmospheric temperature and moisture soundings. The ATMS temperature-sounding channels have exactly the same channel frequencies for most channels, except for channel 4, as its predecessor, the AMSU-A (Table 1). This is a critical feature of the instrument design that allows temperatures of the same atmospheric layers to be measured continuously from the past to the present and onward to the future. With these characteristics, errors due to channel frequency differences are not to be expected between ATMS and AMSU-A, unlike in the case between the first (MSU) and second (AMSU-A) generations of the microwave sounders.

The SNPP satellite was launched on 28 October 2011 onto an afternoon orbit with the ascending LECT at 13:30 p.m. This orbit has been fixed using onboard propulsion at its original time with a drifting error of less than 10 min throughout the SNPP operation from its launch time until the present (Fig. 2). Up to the present, the SNPP/ATMS has more than 6 years of overlapping observations with AMSU-A on several polar-orbiting satellites that are still operational. Among these satellites, the NASA Aqua also has a stable orbit with its ascending LECT fixed at close to 13:30 p.m. throughout its operations since its launch on 4 May 2002 (Fig. 2). In addition, the European MetOp-A has a stable orbit but with a different ascending LECT fixed at close to 21:30 p.m. since its launch on 19 October 2006 (Fig. 2). In operations for more than 10 years

Table 1. Channel frequencies of satellite microwave sounders. Channel frequencies of MSU, AMSU-A, and ATMS. The 51.76 GHz channel is unique to the ATMS sensor. The vertical and horizontal polarizations of the channels are denoted by V and H, respectively. Unit in GHz.

MSU	AMSU-A	ATMS
	23.8 (V), Ch1	23.8 (V), Ch1
	31.4 (V), Ch2	31.4 (V), Ch2
50.3 (V), Ch1	50.3 (V), Ch3	50.3 (H), Ch3
		51.76 (H), Ch4
	52.8 (V), Ch4	52.8 (H), Ch5
53.74 (H), Ch2	53.595 ± 0.115 (H), Ch5	53.596 ± 0.115 (H), Ch6
	54.4 (H), Ch6	54.4 (H), Ch7
54.96 (H), Ch3	54.94 (V), Ch7	54.94 (H), Ch8
	55.5 (H), Ch8	55.5 (H), Ch9
57.95 (H), Ch4	57.290 (H), Ch9	57.290 (H), Ch10
	57.290 ± 0.217 (H), Ch10	57.290 ± 0.217 (H), Ch11
	57.290 ± 0.3222 ± 0.048 (H), Ch11	57.290 ± 0.3222 ± 0.048 (H), Ch12
	57.290 ± 0.3222 ± 0.022 (H), Ch12	57.2903 ± 0.322 ± 0.022 (H), Ch13
	57.290 ± 0.3222 ± 0.010 (H), Ch13	57.290 ± 0.322 ± 0.010 (H), Ch14
	57.290 ± 0.3222 ± 0.0045 (H), Ch14	57.290 ± 0.322 ± 0.0045 (H), Ch15

and far exceeding their 5-year design life, most Aqua and MetOp-A AMSU-A channels are still in excellent working conditions. The fact that SNPP/ATMS and Aqua/AMSU-A have the same local observation time provides an excellent opportunity to examine their radiometric stability, because diurnal drift effects are absent between the two observations during their entire overlapping period.

RESULTS

Assessment of radiometric stability on SNPP/ATMS and Aqua/AMSU-A

We show in Fig. 3 the anomaly time series of brightness temperatures averaged over the ascending and descending orbits for the example channels, SNPP/ATMS channel 9 versus its Aqua/AMSU-A counterpart channel 8, and their difference time series. We also show in fig. S1 (A and B) the global mean anomalies for all analyzed channels here for ascending and descending orbits, respectively. The temperature anomalies in Fig. 3 and fig. S1 are a quantity measuring layer mean temperature changes with respect to a climatology for each individual channel. The temperatures in the climatology are fixed values for each month and each grid cell (fig. S2). As a multiyear mean of the monthly brightness temperatures, the climatology is composed of two parts: the actual climatology representing the real atmosphere measured by the specific channel and calibration biases. The latter quantity may change slightly with season and geolocation, a consequence of scene temperature–dependent biases owing to inaccurate calibration nonlinearity (*10*). These scene temperature–dependent biases are respectively demonstrated in figs. S2 and S3 in the climatology differences between SNPP and Aqua.

Because changes of calibration biases with season have been included in climatology, calibration-drifting error, if it exists, will be reflected in the anomaly time series as change of calibration biases from year to year. We define an observation as being absolutely stable or free of calibration-drifting error if calibration biases do not incur interannual change. For absolute stable observations, the anomaly time series shall represent the actual climate changes in the layer mean temperatures measured by the instrument channels. Calibration-drifting errors are unknown a priori in general, and they can only be identified when the anomaly time series are compared to a reference with known drifting errors. Unfortunately, such a reference does not usually exist. The fact that Aqua/AMSU-A and SNPP/ATMS have the same channel frequencies for most channels and stable orbits with close to the same local observation time provides a rare opportunity for examination of their relative drifting errors and mutual validation.

The difference time series between the SNPP/ATMS and Aqua/AMSU-A anomalies demonstrate favorable statistics on their radiometric stability. For most channels and both ascending and descending orbits, their anomaly differences during their overlaps from December 2011 to April 2018 are less than 0.02 K in all monthly averages with a mean of 0 K to two decimal places and an SD of only around 0.005 to 0.01 K (Fig. 3 and fig. S1). The 6-year trends for the anomaly difference time series are less than 0.04 K per decade for seven of eight channels for both ascending and descending orbits examined here. Trend differences between ascending and descending orbits in the anomaly difference time series are less than 0.01 K per decade for all channels. The high precision in the anomaly difference time series allows their trend estimates with much lower uncertainty, being around 0.02 K per decade for most channels, although the overlapping period is still short. These trend statistics suggest that there are little or nearly no relative drifting errors between the SNPP/ATMS and Aqua/AMSU-A observations. Because the two instruments were calibrated completely independently and no time-dependent intersatellite bias correction was imposed, it is unlikely that their biases are drifting to exactly the same direction to arrive at a near-zero relative drifting error. The most probable explanation is that the anomaly time series from both observations closely represent the actual change of the atmosphere, that is, both instruments have achieved an absolute radiometric stability within 0.04 K per decade.

Such a stability has an important implication for climate trend detection. It suggests that climate temperature trends can be detected with an uncertainty only of 0.04 K per decade from the troposphere to the

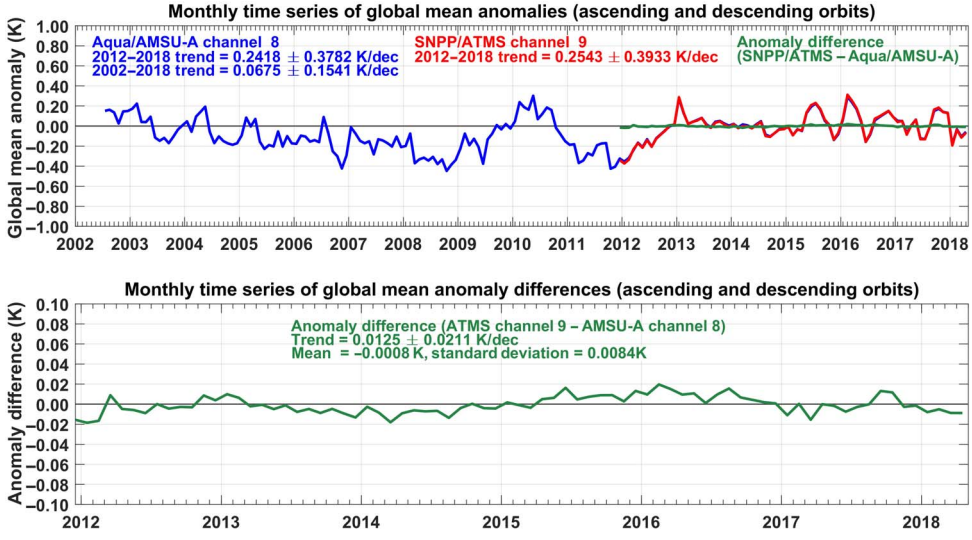

Fig. 3. Anomaly time series for assessment of radiometric stability. Monthly global mean anomaly time series of brightness temperatures for AMSU-A channel 8 onboard Aqua (blue, top) versus ATMS channel 9 onboard SNPP (red, top) and their difference time series (green, top and bottom). The AMSU-A and ATMS data are from June 2002 and December 2011 to April 2018, respectively. The AMSU-A anomaly time series are overlaid by ATMS during their overlapping period, with their differences shown as nearly a constant zero line in the same temperature scale. Amplified scale of temperature is used in the bottom panel to show detailed features in the anomaly difference time series. Both ATMS and AMSU-A data are from limb-adjusted views and averaged over ascending and descending orbits. Uncertainties in trends represent 95% confidence intervals with autocorrelation adjustments.

stratosphere. Given the required instrument stabilities for detecting climate change, which are 0.04 K per decade for the troposphere and 0.08 K per decade for the stratosphere (*21*), the uncertainties we obtained are sufficiently small, especially for the stratospheric channels, for accurate trend determination that could serve as a basic information in advancing climate change science such as understanding past climate changes and validation of climate model simulations to build confidence for climate change prediction in the future. Considering that the overlap between SNPP and Aqua is still short in our current comparison, we expect that the trends in their difference time series, and thus the observational uncertainty in the trend detection, will become yet smaller when both observations become longer.

The only exception is for AMSU-A channel 9 versus ATMS channel 10, which have a trend of 0.06 K per decade in their anomaly difference time series. There are two possible reasons for this larger drift. The first is inaccurate calibration nonlinearity in either of the ATMS or AMSU-A instruments. On the basis of analyses of calibration equation (12) and of simultaneous nadir overpasses for satellite pairs (9-10), inaccurate calibration nonlinearity causes observational biases to depend on scene temperatures in which biases are approximately linearly proportional to differences between the scene and reference temperatures. This is mathematically expressed as

$$\text{Observational biases } = (T_o - T_r) \sim \alpha (T_o - T_0) \qquad (1)$$

where T denotes brightness temperatures and the subscripts o, r, and 0 represent observations, the assumed truth, and a constant reference, respectively; α is a slope that can reach to the order of 0.01 to 0.02 for channels with large inaccuracy in calibration nonlinearity (*9*, *12*). One consequence of the scene temperature–dependent biases is errors in the observed amplitudes of seasonal cycles, which is the primary reason for the seasonally dependent biases in climatology between the SNPP/ATMS and Aqua/AMSU-A observations (fig. S3). By taking the derivative of Eq. 1 with time, the scene temperature–dependent biases also induce errors in the estimates of long-term temperature trends that are approximately linearly proportional to the magnitude of trends observed by the instrument channels.

The second reason is a possible shift in channel frequencies in the comparing instruments. Researchers found frequency shifts for certain AMSU-A channels in previous investigations (*10*, *20*). Channel frequency shift causes an instrument channel to measure temperatures at atmospheric layers differently from its original design. Frequency mismatch between two instrument channels could result in a nonzero trend in their anomaly difference time series being equal to the trend differences between the two layers of the real atmosphere observed by the two channels.

The effects from the above two sources of error appear to be small for most channels in the SNPP and Aqua comparisons, but non-negligible for the exceptional channels. Nevertheless, the exceptional channels measure temperatures in the lower stratosphere, and the magnitude of their relative drift is actually within the required instrument stability of 0.08 K per decade for the stratosphere. In this sense, this exception is not a big concern on the statement of the high radiometric stability performance in the SNPP/ATMS and Aqua/AMSU-A observations. However, the potential impact on the accuracy of trend estimates from these sources of error needs to be carefully examined whenever two instruments are compared for assessment of radiometric stability and when observations from the SNPP/ATMS and Aqua/AMSU-A continue into the future.

Comparisons between SNPP/ATMS and MetOp-A/AMSU-A

It is of interest to understand whether the stability assessment approach above can be applied to satellites with stable orbits but different overpass times such as those between SNPP and MetOp-A. We show in Fig. 4 the temperature anomaly time series for SNPP/ATMS channel 5 and its MetOp-A/AMSU-A counterpart channel 4 as well as their differences for ascending and descending orbits, respectively. These channels measure temperatures of the lower troposphere with a weighting function peaking near 0.5 km (Fig. 1). Figures S4 and S5 show similar comparisons for all analyzed channels for global ocean and global land means, respectively. Similar to the comparisons between SNPP and Aqua, the anomaly differences between SNPP and MetOp-A have means of 0 K to two decimal places for both ascending and descending orbits. However, the SDs for these differences are much larger, ranging from 0.015 K for the tropospheric channels to 0.04 K for the upper stratospheric channels over the global ocean (fig. S4).

Focusing on SNPP/ATMS channel 5 and MetOp-A/AMSU-A channel 4, trends in their anomaly differences show large disagreement between the ascending and descending orbits, being 0.025 K per decade for the former and 0.097 K per decade for the latter, respectively (Fig. 4). This yields a difference as large as 0.072 K per decade between them. This is in contrast to the comparisons between the SNPP and Aqua where trends in their anomaly differences are about the same for ascending and descending orbits for all channels (fig. S1). Because the instrument

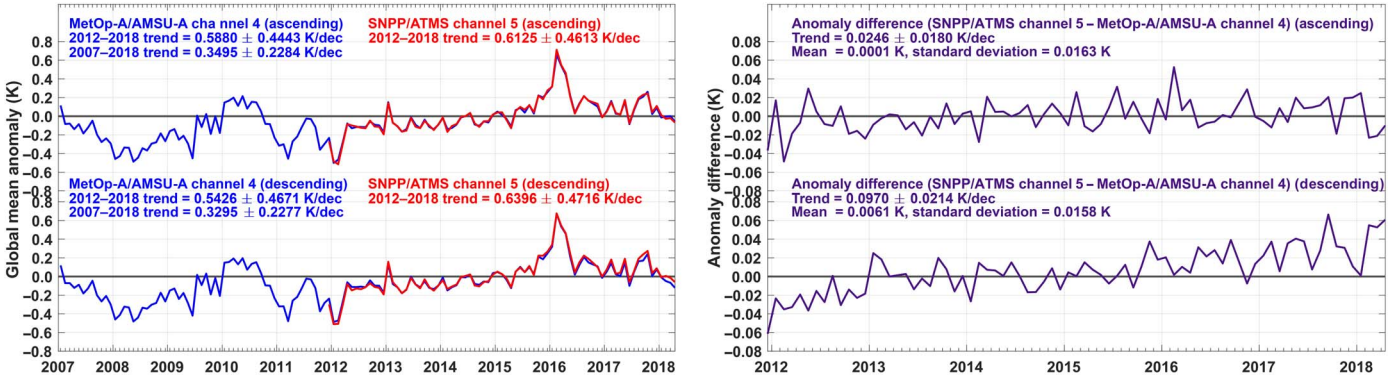

Fig. 4. Anomaly time series for assessment of asymmetric diurnal temperature trends. Monthly global mean anomaly time series of brightness temperatures for AMSU-A channel 4 onboard MetOp-A (blue, left) versus ATMS channel 5 onboard SNPP (red, left) and their difference time series (right). The top and bottom panels are for ascending and descending orbits, respectively. Both ATMS and AMSU-A data are from limb-adjusted views. Uncertainties in trends represent 95% confidence intervals with autocorrelation adjustments.

calibration equation is the same for ascending and descending orbits (9-10), we expect instrument-specific errors, such as instrument calibration drifts, if they exist, to be the same for ascending and descending orbits and thus they cancel out in the differentiations between the two nodes. This is supported by the comparisons between SNPP and Aqua, in which the trend differences between the ascending and descending orbits in their anomaly difference time series are less than 0.01 K per decade for all channels (fig. S1). This argument rules out the calibration drifts and other instrument-specific errors as potential causes for the large trend difference of 0.072 K per decade between the ascending and descending orbits for SNPP and MetOp-A. As a result, the only reason left to explain their dissimilarity in ascending and descending orbits would be their differences in observation time.

Looking at the SNPP and MetOp-A trends during 2012–2018 in Fig. 4 for ascending and descending nodes separately and taking their LECT information into consideration, the MetOp-A nighttime trend at 21:30 a.m. local time from the ascending orbits (0.588 K per decade) was warmer than its daytime trend at 9:30 p.m. local time from the descending orbits (0.543 K per decade) by 0.045 K per decade. Meanwhile, the SNPP nighttime trend at 1:30 a.m. from the descending orbits (0.640 K per decade) was warmer than its daytime trend at 13:30 p.m. from the ascending orbits (0.613 K per decade) by 0.027 K per decade. Note that trend values for a specific ascending or descending node could contain an unknown calibration-drifting error (up to 0.04 K per decade based on the analyses on SNPP and Aqua), but this error mostly cancels out by differentiations between the ascending and descending orbits for the same satellite. Consequently, the trend differences between the daytime and nighttime temperatures are fairly reliable.

In summary of the above analyses, the two daytime observations minus the two nighttime observations from the SNPP and MetOp-A satellites had been cooling at a rate of 0.072 K per decade (=0.045 K per decade + 0.027 K per decade) during 2012–2018. This equals exactly the trend differences between the descending and ascending orbits in the SNPP and MetOp-A anomaly difference time series (=0.097 K per decade − 0.025 K per decade). Note that averages of the two daytimes are close to the local noon, while averages of the two nighttimes are close to the local midnight. This gives an estimated cooling trend of about 0.036 K per decade for the global lower-tropospheric temperature differences of the local noon and local midnight (the former minus the latter), which is one-half of those between the two daytime and two nighttime observations. Such asymmetric trends in the daytime and nighttime temperatures behave differently over the land and ocean. Over the global land, the MetOp-A daytime temperatures at 9:30 a.m. minus its nighttime temperatures at 21:30 p.m. cooled at a rate as large as 0.111 K per decade; over the global ocean, however, this relative cooling was only 0.018 K per decade. Meanwhile, the SNPP daytime temperatures at 13:30 p.m. minus its nighttime temperatures at 1:30 a.m. cooled at a rate of 0.033 K per decade over land and 0.024 K per decade over ocean, respectively. By averaging the SNPP and MetOp-A observations, the estimated cooling trend of the local noon relative to local midnight was about 0.072 K per decade over the global land (which happened to be twice as large as the global means) and 0.021 K per decade over the global ocean.

As an index for diurnal temperature differences, the diurnal temperature range, defined as the differences between the daily maximum and minimum temperatures, was found decreasing at a rate of 0.066 K per decade during 1950–2004 over the global land surface (*22*, *23*). We expect similar cooling trends in diurnal temperature range for satellite temperature of the lower troposphere because it is close to the surface. The cooling trends of the satellite daytime relative to nighttime observations found here for the lower-tropospheric temperatures over the global land resemble the cooling trends in the diurnal temperature range at the surface, although they were estimated for different periods of time from different local observation times.

AMSU-A channel 5 and ATMS channel 6 measure temperatures in the mid-troposphere, which receive a smaller portion of radiative contribution from the surface than AMSU-A channel 4 and ATMS channel 5. As a result, they exhibited similar asymmetric diurnal trends but with smaller magnitudes. Specifically, the MetOp-A daytime temperatures at 9:30 a.m. minus the nighttime temperatures at 21:30 p.m. cooled at a rate of 0.048 K per decade over the global land and 0.010 K per decade over the global ocean, respectively. The SNPP daytime temperature at 13:30 p.m. minus the nighttime temperature at 1:30 a.m. had a cooling trend of 0.015 K per decade over the global land and 0.024 K per decade over the global ocean, respectively. In average, the local noon minus local midnight had an estimated cooling trend of about 0.031 K per decade over the global land and 0.017 K per decade over the global ocean, respectively, for the mid-tropospheric temperatures during 2012–2018.

The existence of asymmetric diurnal temperature trends makes it complicated to use satellite difference time series to assess radiometric stabilities for the surface-affected channels when satellite orbits are separated by a few hours, although they are stable. There is an ambiguity to explain their differences. Large trends in their anomaly differences, as in the case between SNPP and MetOp-A for the descending orbits, do not necessarily suggest large instrument calibration drifts because they could be caused by asymmetry in diurnal temperature trends in the real atmosphere. On the other hand, small trends in the anomaly differences, as in the case between the SNPP and MetOp-A for ascending orbits, do not necessarily suggest small calibration drifts because they could be a cancellation result between large calibration drifts and trends in diurnal temperature differences. Hence, more sophisticated approaches may need to be developed for accurate assessment of instrument stabilities for the surface-affected channels for satellites with different orbits. Nevertheless, satellites in the MetOp series all have the same orbits. The MetOp-A/AMSU-A radiometric stability could be assessed by comparisons with MetOp-B/AMSU-A, which has overlaps since September 2012, using the same approach as for the SNPP and Aqua.

Although radiometric stability cannot be determined for MetOp-A/AMSU-A channels 4 and 5 and SNPP/ATMS channels 5 and 6, orbital differences between them allow reliable estimates of relative trends between the daytime and nighttime temperatures for the lower and middle troposphere. This unique measurement capability would benefit the investigation and understanding of the long-term trends in diurnal temperature range and their relationship to changes in cloud, precipitation, aerosol, soil moisture, temperature extremes, and other atmospheric and surface variables (*24*).

For the stratospheric channels, that is, SNPP/ATMS channels 11 to 15 and MetOp-A/AMSU-A channels 10 to 14 where surface contribution is absent (Fig. 1), asymmetric diurnal temperature trends appeared to be negligible (figs. S4 and S5). Consequently, similar to SNPP and Aqua, the small trends in the anomaly differences between SNPP and MetOp-A for both ascending and descending orbits suggest that both instruments have achieved an absolute radiometric stability within 0.04 K per decade for these stratospheric channels (fig. S4). However, due to the lower precision in the differences between SNPP/ATMS channel 15 and MetOp-A/AMSU-A channel 14, the uncertainty associated with the trend calculation is as high as ±0.07 K per decade for the anomaly differences over the ocean. This resulted in lower reliability on the stability assessment for MetOp-A/AMSU-A channel 14.

Atmospheric temperature trends during 2002–2018 observed from the Aqua/AMSU-A channels

The high radiometric stability performance in Aqua/AMSU-A during its overlaps with SNPP/ATMS can be extended to its earlier observations because the calibration algorithm has been maintained the same throughout the Aqua/AMSU-A operations (*10*). Hence, climate temperature trends from the Aqua/AMSU-A should have an observational uncertainty of 0.04 K per decade for its entire observational period. We summarize in Fig. 5 the 16-year trends for Aqua/AMSU-A channels 7 to 14 during 2002–2018, representing temperatures from the upper troposphere to the upper stratosphere. Although observational uncertainties are small, uncertainties associated with time length and temporal variability are still non-negligible, and they are shown as uncertainty bars superimposed on the trend values. These uncertainties will become smaller as observations become longer. This figure provides a vertical structure of the global temperature trends with high resolution and negligible observational uncertainty. Temperature trends in the upper troposphere were 0.12 ± 0.16 K per decade, gradually decreasing to near zero in the lower stratosphere and cooling with a magnitude of 0.49 ± 0.19 K per decade in the upper stratosphere. This structure is consistent with the recent examinations of atmospheric temperature trends with longer period of satellite observations and climate model simulations (*25*).

DISCUSSION

The high radiometric stability in the SNPP/ATMS and Aqua/AMSU-A measurements, as well as the MetOp-A/AMSU-A stratospheric channels, has broad impact on the climate trend observations from the microwave sounders as well as other instruments and could help resolve debates on observed differences in the climate trends. Radiosonde observations had been homogenized and extensively used for detecting climate temperature trends from the lower troposphere to the lower stratosphere (*8*, *26*–*31*). Researchers found disagreement in climate trends between the satellite and radiosonde observations (*32*, *33*). It remains a puzzle so far as to determine which of the two observations are more reliable when their derived trends in the atmospheric temperatures differ. By comparing with the stable observations from the SNPP/ATMS and Aqua/AMSU-A, biases and their drifts over time in the radiosonde observations could be identified, which could, in turn, help in developing more accurate radiosonde data records for climate trend detection.

Similarly, the GPS radio occultation (RO) observations had been used for temperature trend investigation over the stratosphere, and they were found in agreement with the Aqua/AMSU-A observations within 0.04 K per decade (*34*). These studies suggested high stability in both the GPS-RO and Aqua/AMSU-A observations for reliable trend detection. In contrast, homogenized satellite data products of earlier versions developed by different research groups showed climate trend differences up to 0.2 K per decade relative to the GPS-RO observations for the lower-stratospheric layer (*35*, *36*). This may suggest potential errors in the applied algorithms in removing diurnal sampling drift or calibration drift when constructing satellite data records of the earlier versions. In this aspect, the stable SNPP/ATMS and Aqua/MetOp-A observations could help in identifying potential drifts in the homogenized satellite temperature records and improve their accuracy by serving as a reference in developing algorithms for corrections of diurnal sampling and calibration-drifting errors. In the latest development of homogenized satellite temperature records, researchers had used Aqua and MetOp-A as references to correct diurnal sampling drifting errors (*13*, *16*). These approaches resulted in better agreement in derived climate trends between some of the latest versions of the homogenized satellite temperature records (*17*, *18*).

Asymmetric trends of diurnal temperatures in the lower and middle troposphere found in the SNPP and MetOp-A observations could bring complications to the selection of the reference satellites for diurnal drift correction and affect the long-term trends in homogenized temperature time series. In developing satellite data records, researchers adjusted satellite observations at different times to either local midnight (*13*) or local noon (*10*, *16*), in which satellites with stable orbits but different overpass times were combined together to serve as references. Over the global land, however, the midnight warms faster than the noon by about 0.072 K per decade and 0.031 K per decade in the lower- and mid-tropospheric temperatures, respectively. In extreme cases, the evening (21:30 p.m.) warms faster than the morning (9:30 a.m.) by as large as 0.111 K per decade for the lower-tropospheric temperatures over land.

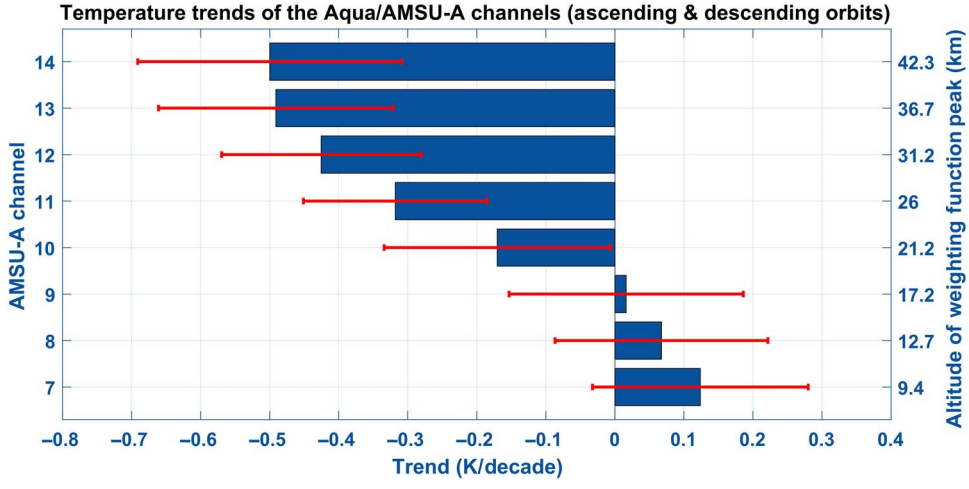

Fig. 5. Atmospheric temperature trends during 2002–2018. Temperature trends during 2002–2018 estimated from Aqua/AMSU-A channels 7 to 14 for averages of ascending and descending orbits, representing temperatures from the upper troposphere to the upper stratosphere. Uncertainties due to time length limitation and temporal variability (not the observational uncertainty due to instability) at 95% confidence intervals with autocorrelation adjustments are superimposed on the trend bars.

For an accurate estimation and fair comparison of long-term trends, different satellite data records should be adjusted to the same local time with asymmetric trends of diurnal temperatures accounted for when conducting diurnal drift corrections. These adjustments require knowledge of the relative trends between different reference satellites. The approach applied in this study for assessing asymmetric trends of diurnal temperatures would help improve the consistency of climate data records for temperature trend detection with improved accuracy.

Last, the assessment approach of radiometric stability and asymmetric diurnal trends using satellites with stable orbits could be applied to satellite microwave humidity sounders, which suffer diurnal sampling and calibration drifts similar to the microwave temperature sounders (*37*). Using humidity measurements from satellites with stable orbits as a reference could potentially help improve the accuracy of bias correction algorithms for more reliable climate change detection in the atmospheric moisture fields.

In conclusion, the next-generation U.S. microwave sounder, the SNPP/ATMS, because of its high accuracy and stable orbit, has brought a highly needed capability in terms of reliably measuring the global and regional climate temperature trends. Such a capability is a critical milestone in resolving debates on uncertainties in the climate's atmospheric temperature trends. The SNPP and NOAA-20 satellites will be followed by three NOAA operational JPSS satellites providing accurate and stable measurement for decades to come. The primary mission of JPSS is for weather forecasting. Now with the added feature of stable orbits, JPSS observations can also be used to monitor changes in climate with much lower uncertainty than the previous generation of NOAA operational satellites. This will benefit the entire climate science and service community for climate change investigation and support of decision-making process on climate change mitigation and adaptation.

MATERIALS AND METHODS

The Aqua and MetOp-A AMSU-A data

The AMSU-A was designed to measure the vertical temperature profile from the Earth's surface to the upper stratosphere with its 15 channels ranging from 23.8 to 89 GHz (Table 1). The AMSU-A is a total power, line-scanning radiometer with an instantaneous field of view (FOV) of 3.3° at the half-power points. Its antenna provides a cross-track scan, covering 48.33° on each side of the nadir direction with a total of 30 Earth FOVs per scan line. These scan patterns and geometric resolution translate to a 45-km-diameter cell at nadir and a 2343-km swath width on the ground from the 833-km nominal orbital altitude.

We used the Aqua and MetOp-A AMSU-A daily gridded brightness temperature data archived at the NOAA/National Centers for Environmental Information (NCEI) in the Climate Data Record Program (https://ncdc.noaa.gov/cdr/fundamental) to generate temperature anomaly time series. The dataset was originally produced by the NOAA/Center for Satellite Applications and Research (STAR) group as an AMSU-A fundamental climate data record (*38*). In this dataset, intersatellite biases were minimized for the AMSU-A observations onboard multiple polar-orbiting satellites, including NOAA-15 to NOAA-18, Aqua, and MetOp-A. For Aqua, only a constant offset was added to its original swath radiances for each individual channel to minimize its differences from AMSU-A observations from other satellites (*10*). In this sense, this version of the Aqua data preserved the characteristics in the original operational calibration in terms of calibration drift, that is, no additional calibration drift was introduced to the Aqua data by the intercalibration effort. For MetOp-A AMSU-A, constant offsets and optimal nonlinear calibration coefficients were applied to minimize its differences from other satellites. Different calibration nonlinearity affects the seasonal cycles observed by the AMSU-A channels (*10*). It may also affect the observed climate trends that are expected to be more reliable with optimal calibration nonlinearity. Uncertainties associated with this effect are discussed in the analysis section.

In addition to swath radiances at each scan angles, the NOAA/STAR AMSU-A fundamental climate data record contains limb-corrected brightness temperatures for Aqua, MetOp-A, and other satellites. A limb correction adjusts radiances at off-nadir view angles to those at the nadir direction. This adjustment allows the use of the off-nadir footprints in the same way as the nadir observations to increase observational samples and reduce noise and sampling-related biases in developing climate data record. The statistical algorithm developed by Goldberg *et al.* (*39*) was used for the AMSU-A limb adjustment, adjusting a target channel using adjacent channels. The NOAA/STAR AMSU-A daily gridded data were generated by accumulating and binning limb-adjusted AMSU-A brightness temperatures into grid cells with a resolution of 1° latitude by 1° longitude and then averaging them in daily intervals (*38*). Among the 30 FOVs in a scan line, only footprints from the scan positions 8 to 23 were used in the daily gridded products, because limb adjustments for these scan positions resulted in off-nadir biases of only 0.1 K (*38*, *40*).

The Aqua and MetOp-A AMSU-A daily data contain files with ascending and descending orbits separately. We further averaged these daily data to derive ascending and descending monthly data with the same spatial resolution. We then calculated a multiyear average for each channel, which is referred to as the annual mean "climatology" throughout this study, for ascending and descending orbits separately and for their averages, by averaging data for the same month at each grid cell through the period from January 2012 to December 2016 (figs. S2 and S3). The period for this climatology is exactly the same as for the ATMS. This is important, as selection of different periods for climatology calculation will introduce signals not suitable for an apple-to-apple comparison of the anomaly time series. Temperature anomalies for ascending and descending orbits and for their averages were calculated for each grid cells based on their climatology. Global mean anomalies were an area-weighted average of the anomalies over the globe for ascending and descending orbits and their averages, respectively.

The archiving in NOAA/NCEI contains AMSU-A data from channels 4 to 14. Aqua AMSU-A channels 4 and 5 failed since September 2007 and April 2012, respectively. The failure in channel 5 affected the quality of limb adjustment for its adjacent channel 6. Therefore, we only compared Aqua/AMSU-A channels 7 through 14 to the ATMS data. Similarly, MetOp-A AMSU-A channels 7 and 8 failed since December 2009 and April 2016, respectively. The failure of these two channels caused quality issues for limb adjustments for their adjacent channels 6 and 9. As a result, we only compared MetOp-A/AMSU-A channels 4, 5, and 10 through 14 to the ATMS data.

SNPP ATMS data

The ATMS is a total power cross-track radiometer with 22 channels, providing sounding observations of the atmospheric temperature and moisture profiles. The ATMS temperature-sounding channels have exactly the same channel frequencies as AMSU-A for most channels except for an addition of channel 4 (51.74 GHz, Table 1) for the measurement of near-surface temperatures. ATMS scans Earth within the range of 52.725° on each side of the nadir direction with an angular sampling interval of 1.11°, providing 96 Earth observations in a scan line. The ATMS

antenna beam width is 2.2° for temperature-sounding channels 3 to 16. The differences in the beam width between ATMS and AMSU-A result in differences in the size of their FOVs. Because the angular sampling interval is much smaller than the beam width, the ATMS scans result in oversampling in both cross-track and along-track directions. A single FOV of any of ATMS channels 3 to 16 typically overlaps with its three neighboring FOVs and three nearby scan lines (*41*). The oversampling in the ATMS observations offers an advantage in the generation of the climate data record—sampling noise can be much reduced when multiple samples are averaged together to generate a single observation to represent a climate state.

We used the SNPP/ATMS temperature data record (TDR) reprocessed by the NOAA/STAR ATMS calibration and reprocessing teams to generate the ATMS anomaly time series. The reprocessed TDR data were generated on the basis of a consistent calibration algorithm as described by Weng *et al.* (*42*). The reprocessing had eliminated radiance discontinuity on March 2017 caused by changes in calibration algorithms during operational processing. The reprocessed TDR contains ATMS brightness temperatures at each scan position. Before using them for stability assessment, we further performed limb adjustments to the ATMS radiance data using limb correction coefficients developed by Zhang *et al.* (*43*). This adjustment resulted in off-nadir biases of only 0.2 K for all off-nadir footprints.

We calculated ATMS monthly anomaly time series similar to AMSU-A for their comparisons and stability assessments. For this purpose, we first generated daily gridded data, for ascending and descending orbits separately, by accumulating and binning limb-adjusted ATMS brightness temperatures into grid cells with a resolution of 1° latitude by 1° longitude and then averaging them in daily intervals. Each ATMS scan has 96 footprints; however, we only used near-nadir footprints from scan positions 29 to 68 to match with the swath width of AMSU-A. To compare with AMSU-A data of the same quantity, we further averaged these daily data in monthly intervals to derive monthly ascending and descending data with the same grid resolution. We calculated temperature anomalies for ascending and descending orbits and for their averages for each grid cells based on their annual mean climatology from January 2012 to December 2016. In figs. S2 and S3, we show comparisons of the ascending and descending climatology to those from Aqua AMSU-A. Similar to AMSU-A, global mean anomalies were an area-weighted average over the anomalies on all grid cells for a specific month.

We performed quality control to ensure that sufficient observations were available for each month in the ATMS and AMSU-A comparisons. After examining all ATMS and AMSU-A monthly data, we found a large amount of missing values in the October 2016 ATMS data and thus removed this month in the comparison.

SUPPLEMENTARY MATERIALS

Supplementary material for this article is available at http://advances.sciencemag.org/cgi/content/full/4/10/eaau0049/DC1

Fig. S1. Anomaly time series for assessment of radiometric stability for all analyzed SNPP/ATMS and Aqua/AMSU-A channels.

Fig. S2. Climatology of upper-tropospheric temperature in April.

Fig. S3. Global mean climatology for all analyzed SNPP/ATMS and Aqua/AMSU-A channels.

Fig. S4. Anomaly time series for assessment of radiometric stability and asymmetric diurnal temperature trends over ocean for all analyzed SNPP/ATMS and MetOp-A/AMSU-A channels.

Fig. S5. Anomaly time series for assessment of radiometric stability and asymmetric diurnal temperature trends over land for all analyzed SNPP/ATMS and MetOp-A/AMSU-A channels.

REFERENCES AND NOTES

1. A. C. Lorenc, R. T. Marriott, Forecast sensitivity to observations in the Met Office Global NWP system. *Q. J. R. Meteorol. Soc* **140**, 209–224 (2014).
2. R. W. Spencer, J. R. Christy, Precision and radiosonde validation of satellite gridpoint temperature anomalies Part I: MSU channel 2. *J. Clim.* **5**, 847–857 (1992).
3. R. W. Spencer, J. R. Christy, Precision and radiosonde validation of satellite gridpoint temperature anomalies Part II: Tropospheric retrieval and trends during 1979–90. *J. Clim.* **5**, 858–866 (1992).
4. J. Hansen, H. Wilson, M. Sato, R. Ruedy, K. Shah, E. Hansen, Satellite and surface temperature data at odds? *Clim. Chang.* **30**, 103–117 (1995).
5. Q. Fu, C. M. Johanson, S. G. Warren, D. J. Seidel, Contribution of stratospheric cooling to satellite-inferred tropospheric trends. *Nature* **429**, 55–58 (2004).
6. K. E. Trenberth, J. W. Hurrell, How accurate are satellite 'thermometers'? *Nature* **389**, 342–343 (1997).
7. F. J. Wentz, M. C. Schabel, Effects of satellite orbital decay on satellite-derived lower-tropospheric temperature trends. *Nature* **394**, 661–664 (1998).
8. J. R. Christy, R. W. Spencer, W. D. Braswell, MSU tropospheric temperatures: Dataset construction and radiosonde comparisons. *J. Atmos. Oceanic Technol.* **17**, 1153–1170 (2000).
9. C.-Z. Zou, M. Goldberg, Z. Cheng, N. C. Grody, J. T. Sullivan, C. Cao, D. Tarpley, Recalibration of microwave sounding unit for climate studies using simultaneous nadir overpasses. *J. Geophys. Res.* **111**, 1–24 (2006).
10. C.-Z. Zou, W. Wang, Inter-satellite calibration of AMSU-A observations for weather and climate applications. *J. Geophys. Res.* **116**, 1–20 (2011).
11. C. A. Mears, M. C. Schabel, F. J. Wentz, A reanalysis of the MSU channel 2 tropospheric temperature record. *J. Clim.* **16**, 3650–3664 (2003).
12. C. A. Mears, F. J. Wentz, Construction of the remote sensing systems v3.2 atmospheric temperature records from the MSU and AMSU microwave sounders. *J. Atmos. Oceanic Technol.* **26**, 1040–1056 (2009).
13. C. A. Mear, F. J. Wentz, 2016: Sensitivity of satellite-derived tropospheric temperature trends to the diurnal cycle adjustment. *J. Clim.* **29**, 3629–3646 (2016).
14. S. Po-Chedley, Q. Fu, A bias in the midtropospheric channel warm target factor on the NOAA-9 Microwave Sounding Unit. *J. Atmos. Oceanic Technol.* **29**, 646–652 (2012).
15. J. R. Christy, R. W. Spencer, W. B. Norris, W. D. Braswell, Error estimates of version 5.0 of MSU-AMSU bulk atmospheric temperature. *J. Atmos. Oceanic Technol.* **20**, 613–629 (2003).
16. S. Po-Chedley, T. J. Thorsen, Q. Fu, Removing diurnal cycle contamination in satellite-derived tropospheric temperatures: Understanding tropical tropospheric trend discrepancies. *J. Clim.* **28**, 2274–2290 (2015).
17. B. D. Santer, S. Solomon, G. Pallotta, C. Mears, S. Po-Chedley, Q. Fu, F. J. Wentz, C.-Z. Zou, J. F. Painter, I. Cvijanovic, C. Bonfils, Comparing tropospheric warming in climate models and satellite data. *J. Clim.* **30**, 373–392 (2017).
18. B. D. Santer, J. C. Fyfe, G. Pallottal, G. M. Flato, G. A. Meehl, M. H. England, E. Hawkins, M. E. Mann, J. F. Painter, C. Bonfils, I. Cvijanovic, C. Mears, F. J. Wentz, S. Po-Chedley, Q. Fu, C.-Z. Zou, Causes of differences in model and satellite tropospheric warming rates. *Nat. Geosci.* **10**, 478–485 (2017).
19. S. Manabe, R. T. Wetherald, Thermal equilibrium of the atmosphere with a given distribution of relative humidity. *J. Atmos. Sci.* **24**, 241–259 (1967).
20. Q. Lu, W. Bell, Characterizing channel center frequencies in AMSU-A and MSU microwave sounding instruments. *J. Atmos. Oceanic Technol.* **31**, 1713–1732 (2014).
21. G. Ohring, B. Wielicki, R. Spencer, B. Emery, R. Datla, Satellite instrument calibration for measuring global climate change. *Bull. Am. Meteorol. Soc.* **86**, 1303–1314 (2005).
22. D. R. Easterling, B. Horton, P. D. Jones, T. C. Peterson, T. R. Karl, D. E. Parker, M. J. Salinger, V. Razuvayev, N. Plummer, P. Jamason, C. K. Folland, Maximum and minimum temperature trends for the globe. *Science* **277**, 364–367 (1997).
23. R. S. Vose, D. R. Easterling, B. Gleason, Maximum and minimum temperature trends for the globe: An update through 2004. *Geophys. Res. Lett.* **32**, 1–5 (2005).
24. T. R. Karl, P. D. Jones, R. W. Knight, G. Kukla, N. Plummer, V. Razuvayev, K. P. Gallo, J. Lindseay, R. J. Charlson, T. C. Peterson, A new perspective on recent global warming: Asymmetric trends of daily maximum and minimum temperatures. *Bull. Am. Meteorol. Soc.* **14**, 1007–1023 (1993).
25. W. J. Randel, L. Polvani, F. Wu, D. E. Kinnison, C.-Z. Zou, C. Mears, Troposphere-stratosphere temperature trends derived from satellite data compared with ensemble simulations from WACCM. *J. Geophys. Res. Atmos.* **122**, 9651–9667 (2017).
26. D. E. Parker, M. Gordon, D. P. N. Cullum, D. M. H. Sexton, C. K. Folland, N. Rayner, A new gridded radiosonde temperature data base and recent temperature trends. *Geophys. Res. Lett.* **24**, 1499–1502 (1997).
27. L. Haimberger, Homogenization of radiosonde temperature time series using innovation statistics. *J. Clim.* **20**, 1377–1403 (2007).
28. L. Haimberger, C. Tavolato, S. Sperka, Towards the elimination of warm bias in historic radiosonde records—Some new results from a comprehensive intercomparison of upper air data. *J. Clim.* **21**, 4587–4606 (2008).

29. L. Haimberger, C. Tavolato, S. Sperka, Homogenization of the global radiosonde temperature dataset through combined comparison with reanalysis background series and neighboring stations. *J. Clim.* **25**, 8108–8131 (2012).
30. S. C. Sherwood, N. Nishant, Atmospheric changes through 2012 as shown by iteratively homogenized radiosonde temperature and wind data (IUKv2). *Environ. Res. Lett.* **10**, 054007 (2015).
31. J. R. Christy, W. B. Norris, Satellite and VIZ–radiosonde intercomparisons for diagnosis of nonclimatic influences. *J. Atmos. Oceanic Technol.* **23**, 1181–1194 (2006).
32. P. W. Thorne, J. R. Lanzante, T. C. Peterson, D. J. Seidel, K. P. Shine, Tropospheric temperature trends: History of an ongoing controversy. *WIREs Clim. Chang.* **2**, 66–88 (2010).
33. D. J. Seidel, N. P. Gillett, J. R. Lanzante, K. P. Shine, P. W. Thorne, Stratospheric temperature trends: Our evolving understanding. *WIREs Clim. Chang.* **2**, 592–616 (2011).
34. S. M. Khaykin, B. M. Funatsu, A. Hauchecorne, S. Godin-Beekmann, C. Claud, P. Keckhut, A. Pazmino, H. Gleisner, J. K. Nielsen, S. Syndergaard, K. B. Lauritsen, Post-millennium changes in stratospheric temperature consistently resolved by GPS radio occultation and AMSU observations. *Geophys. Res. Lett.* **44**, 7510–7518 (2017).
35. S.-P. Ho, Y.-H. Kuo, Z. Zeng, T. C. Peterson, A comparison of lower stratosphere temperature from microwave measurements with CHAMP GPS RO data. *Geophys. Res. Lett.* **34**, 1–5 (2007).
36. A. K. Steiner, B. C. Lackner, F. Ladstädter, B. Scherllin-Pirscher, U. Foelsche, G. Kirchengast, GPS radio occultation for climate monitoring and change detection. *Radio Sci.* **46**, 1–17 (2011).
37. A. Kottayil, V. O. John, S. Buehler, Correcting diurnal aliasing in satellite microwave humidity sounder measurements. *J. Geophys. Res. Atmos.* **118**, 101–113 (2013).
38. C.-Z. Zou, W. Wang, X. Hao, *AMSU Brightness Temperature—NOAA and AMSU Brightness Temperature—NOAA Gridded, Climate Algorithm Theoretical Basis Document, Revision 2, CDRP-ATBD-0345* (NOAA/NESDIS, 2016); https://www1.ncdc.noaa.gov/pub/data/sds/cdr/CDRs/AMSU%20Brightness%20Temperatures/AlgorithmDescription_01B-18_18a.pdf.
39. M. D. Goldberg, D. S. Crosby, L. Zhou, The limb adjustment of AMSU-A observations: Methodology and validation. *J. Appl. Meteorol.* **40**, 70–83 (2001).
40. W. Wang, C.-Z. Zou, AMSU-A-only atmospheric temperature data records from the lower troposphere to the top of the stratosphere. *J. Atmos. Oceanic Technol.* **31**, 808–825 (2014).
41. X. Zou, F. Weng, H. Yang, Connecting the time series of microwave sounding observations from AMSU to ATMS for long-term monitoring of climate. *J. Atmos. Oceanic Technol.* **31**, 2206–2222 (2014).
42. F. Weng, X. Zou, N. Sun, H. Yang, M. Tian, W. J. Blackwell, X. Wang, L. Lin, K. Anderson, Calibration of Suomi national polar-orbiting partnership advanced technology microwave sounder. *J. Geophys. Res. Atmos.* **118**, 11187–11200 (2013).
43. K. Zhang, L. Zhou, M. Goldberg, X. Liu, W. Wolf, C. Tan, Q. Liu, A methodology to adjust ATMS observations for limb effect and its applications. *J. Geophys. Res. Atmos.* **122**, 11347–11356 (2017).

Acknowledgments: We thank L. Flynn, I. Csiszar, and the two anonymous reviewers for providing useful comments that helped improve the manuscript. We thank K. Zhang and L. Zhou for providing the limb adjustment coefficients for the SNPP/ATMS. The ATMS data were provided by the NOAA/STAR ATMS SDR, ICVS, and reprocessing teams. **Funding:** This study was supported by NOAA grant NESDIS-NESDISPO-2009-2001589 (SDS-09-15) and the NOAA's Climate Program Office, Climate Monitoring Program.
Author contributions: C.-Z.Z. and M.D.G. designed the research and wrote the manuscript. X.H. processed satellite data. All authors reviewed the manuscript.
Competing interests: The authors declare that they have no competing interests.
Data and materials availability: All data needed to evaluate the conclusions in the paper are present in the paper and/or the Supplementary Materials. Additional data related to this paper may be requested from the authors. The views, opinions, and findings contained in this report are those of the authors and should not be construed as an official NOAA or U.S. Government position, policy, or decision.

Submitted 26 April 2018
Accepted 10 September 2018
Published 17 October 2018
10.1126/sciadv.aau0049

Citation: C.-Z. Zou, M. D. Goldberg, X. Hao, New generation of U.S. satellite microwave sounder achieves high radiometric stability performance for reliable climate change detection. *Sci. Adv.* **4**, eaau0049 (2018).